Journal of Alloys and Compounds 480 (2009) 537–540

Contents lists available at ScienceDirect

Journal of Alloys and Compounds

journal homepage: www.elsevier.com/locate/jallcom

Phase transition and IR properties of tungsten-doped vanadium dioxide nanopowders

Zifei Peng*, Yuan Wang, Yanyun Du, Dan Lu, Dazhi Sun

Department of Chemistry, Shanghai Normal University, Guilin Road 100, Shanghai, 200234, PR China

ARTICLE INFO

Article history:
Received 7 December 2008
Accepted 24 January 2009
Available online 6 February 2009

Keywords:
Composite materials
Chemical synthesis
Optical properties
Optical spectroscopy

ABSTRACT

Thermochromic vanadium dioxide exhibits a semiconducting to metallic phase transition at $T_t = 341$ K, involving strong variations in electrical, magnetic, optical transmittance. Tungsten-doped vanadium dioxide nanopowders were synthesized by thermolysis with slight improvement and active white powdery tungstic acid (WPTA) used as a substitutional dopant. The results show that the phase transition temperature of the doped VO_2 powders were decreased to 298.6 K, which is very close to the room temperature. Tungsten-doped has enhanced the IR properties of VO_2 nanopowders because the contrast of its IR transmission below and above the room temperature is up to 92% in our experiment.

1. Introduction

Vanadium oxides compounds (V_2O_3, V_2O_5, V_6O_{13}, etc.) present a first order phase transition [1] and exhibit a semiconducting to metallic phase transition at their transition temperatures, involving strong variations in electrical, magnetic, optical transmittance in the infrared region. Among these oxides, VO_2 has attracted much attention and been extensively studied [1–3], because its transition temperature, T_t, is close to room temperature ($T_t < 341$ K) [4]. And it can be considered as a very good candidate for a lot of switching applications: thermal sensors, smart IR optical windows [5–7], smart IR emissive coatings [8], and switching electrical resistances [9].

The VO_2 material, for example, exhibits infrared transmission with a monoclinic structure at $T < T_t$, where T is the ambient temperature. It becomes, however, infrared reflection and has a tetragonal rutile structure at $T > T_t$. According to described above, it is required for a smart window. In winter, it allows infrared solar transmittance and keeps the indoor warm; in summer, the smart window VO_2 coating blocks infrared solar transmittance and makes the indoor cool. In addition, a "smart window" used in international safeguard satellites could help protect sensitive optical surveillance systems from accidental damage or even sabotage [10]. If we could make use of VO_2 for the smart windows and in automobiles, electricity consumption can be lowered by 30%, as well as other fuels conserved [11–13], because about 50% of the total solar energy is distributed to the infrared spectral range.

To make VO_2 effective as an intelligent window material, it is desirable to lower the transition temperature from 341 K to near room temperature for practical applications [11–15]. Doping studies have shown that the transition temperature can be altered by the incorporation of metal ions into the VO_2 lattice [16,17]. It has been found that the most effective metal ion is tungsten [18], because it produces reversely large T_t shifts for small dopant concentrations [19].

In this paper, we have slightly improved the method of thermolysis to prepare tungsten-doped vanadium dioxide nanopowders using white powdery tungstic acid (WPTA) as the dopant. The process can be easily applied to commercial production lines due to its short cycle period and simple operation, and obtained a better result to reduce transition temperature. We have reduced the phase transition temperature to 298.6 K, which is very close to room temperature. And at 293 K and 303 K, the contrast of the semi-metal states of the transmittance(ΔT) is measured being 92%. Such doped VO_2 nanopowders have a potential to be used as smart windows materials.

2. Experimental

Undoped and tungsten-doped vanadium dioxide were prepared by the reference [20]. We slightly improved the method. Hydrazine hydrogen chloride was added with less amount (1.00 g) and without solution when prepare vanadyl chloride ($VOCl_2$) solution.15 g ammonium bicarbonate (NH_4HCO_3) was dropped into the $VOCl_2$ solution with stirring (as the VO^{2+} is stable in the acidity condition) when prepare the precursor of nanopowders.

* Corresponding author. Tel.: +86 21 64322513; fax: +86 21 64322511.
E-mail address: peng1133@shnu.edu.cn (Z. Peng).

0925-8388/$ – see front matter © 2009 Elsevier B.V. All rights reserved.
doi:10.1016/j.jallcom.2009.01.092

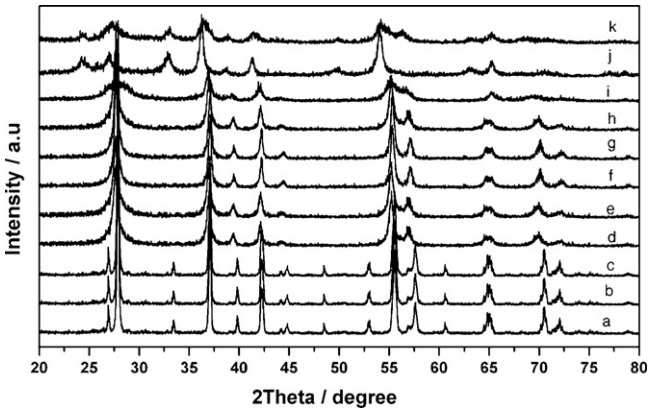

Fig. 1. XRD patterns of VO_2 particles with different tungsten-doping fractions: (a) 0%, (b) 1.07%, (c) 2.13%, (d) 3.01%, (e) 4.11%, (f) 5.07%, (g) 6.15%, (h) 7.21%, (i) 8.02%, (j) 9.13% and (k) 10.03% (calcinations condition: 773 K for 0.5 h).

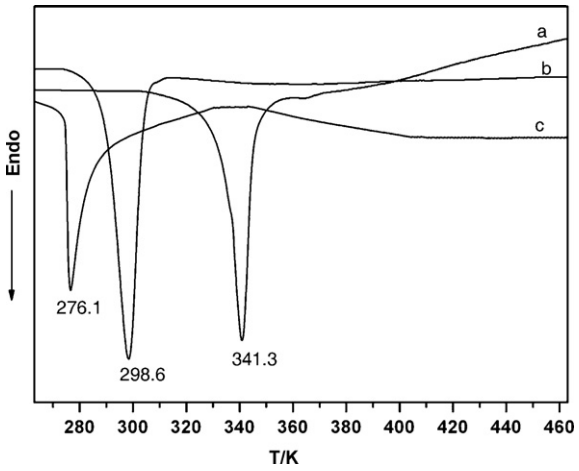

Fig. 2. DSC results of VO_2 with different WPTA-doping contents: (a) 0%, (b) 2.13%, (c) 8.02%.

3. Results and discussion

3.1. X-ray diffraction analyses

The XRD patterns of W-doped VO_2 particles with various W contents are presented in Fig. 1. It can be seen from Fig. 1that all the W-doped VO_2 are well crystallized and consistent with JCPDS 43-1051, even the W atomic percent is up to 7.21%. But for powders with dopant level higher than 8.02%, extra reflections are seen in the X-ray diffraction patterns which do not correspond to any vanadium oxide phase. This is most likely because some of the tungsten go towards the formation of tungsten oxides. It illuminates that 8.02% is a crunode for W-doped VO_2 particles, which consists with the report that tungsten dopant would restrain the growth of VO_2 crystal [21].

Vanadium dioxide is a thermochromic compound showing a reversible metal–semiconductor phase transition at a temperature T_t. Above T_t it has a tetragonal rutile structure and exhibits metallic properties, while below T_t it is a semiconductor with a monoclinic structure. From Fig. 1, we can see that the small reflection angle at 26.7° could not be found when W content is above 3.01%, suggesting that the thermal transition was observed from changed of the monoclinic structure to tetragonal rutile structure. This indicates that the transition temperature in our samples (from 3.01% to 8.02%) is below room temperature, which is in accord with the differential scanning calorimetry (DSC) data.

According to the results of seven crystalline samples calculated by the Scherrer equation, the powder sizes are 10–20 nm, which corresponded to those of TEM.

3.2. Thermal studies

DSC experiments were performed to determine the phase transition temperature of the sample. The typical DSC curves of the W-doped particles with various W fractions between 263 K and 473 K are manifested in Fig. 2. The T_t is significantly decreased from 341.3 K to 298.6 K, which is near room temperature. A noticeable endothermal profile is exhibited in the DSC curve when the phase transition of VO_2 occurs. The temperature on this endothermal peak corresponds to that of the VO_2 phase change. It could be seen that the T_t of undoped VO_2 particles is 341.3 K (the peak temperature), very close to 341 K, which was reported by Morin [4]. When tungsten atoms were doped, the T_t decreased respectively to 298.6 K and 276.1 K for samples with 2.13% and 8.02% of W atomic.

Thus, Fig. 3 also shows the transition temperature versus tungsten atom percent incorporation, and suggests that the phase transition of W-doped VO_2 nanopowders declined with increasing W-doping content. We can see that the curve in Fig. 3 can be divided into two parts: one part shows that the phase transition temperature sharply decreased to 288.4 K when the W atomic percent is up to 3.01% W, decreasing by 17.6 K with every 1% W doping; the other part displays that the transition temperature changed a little when a dopant level above 3.01%. Indeed, some authors have proposed that tungsten dopant would restrain the growth of VO_2 crystal [21]. And Tang et al. [22] has concluded that each tungsten ion in the VO_2 lattice breaks up a V^{4+}–V^{4+} homopolar bond. For charge compensation, two W 3d electrons are transferred to a nearest neighbour vanadium ion to form a V^{3+}–W^{6+} and a V^{3+}–V^{4+} pair. The loss of homopolar V^{4+}–V^{4+} bonding destabilizes the semiconducting phase and lowers the metal–semiconductor transition temperature [22,23]. Both groups of authors have described the doping effect of tungsten [22] on VO_2 in terms of a local model in which coupled pairs of ions have definite valences and form local paramagnetic moments. Nevertheless, the phase transition is a collective phenomenon and the doped VO_2 is believed to consist of weakly interacting magnetic regions in the case of tungsten doping [22].

3.3. X-ray photoelectron spectroscopy analyses

The valence state and content of vanadium and tungsten were studied by XPS. Fig. 4 shows the typical XPS valence band spectra

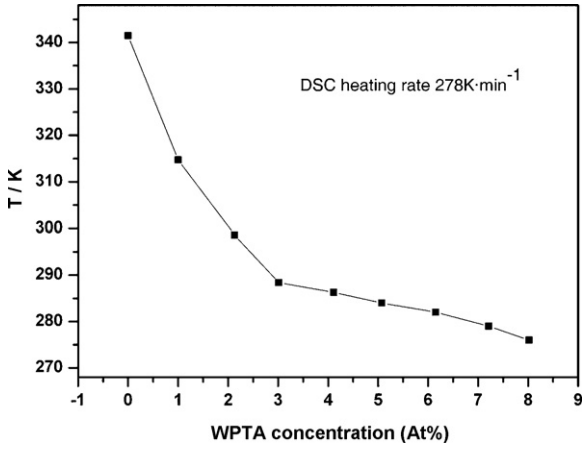

Fig. 3. Relationship between phase transition temperature of the samples and WPTA doped concentration in VO_2 particles.

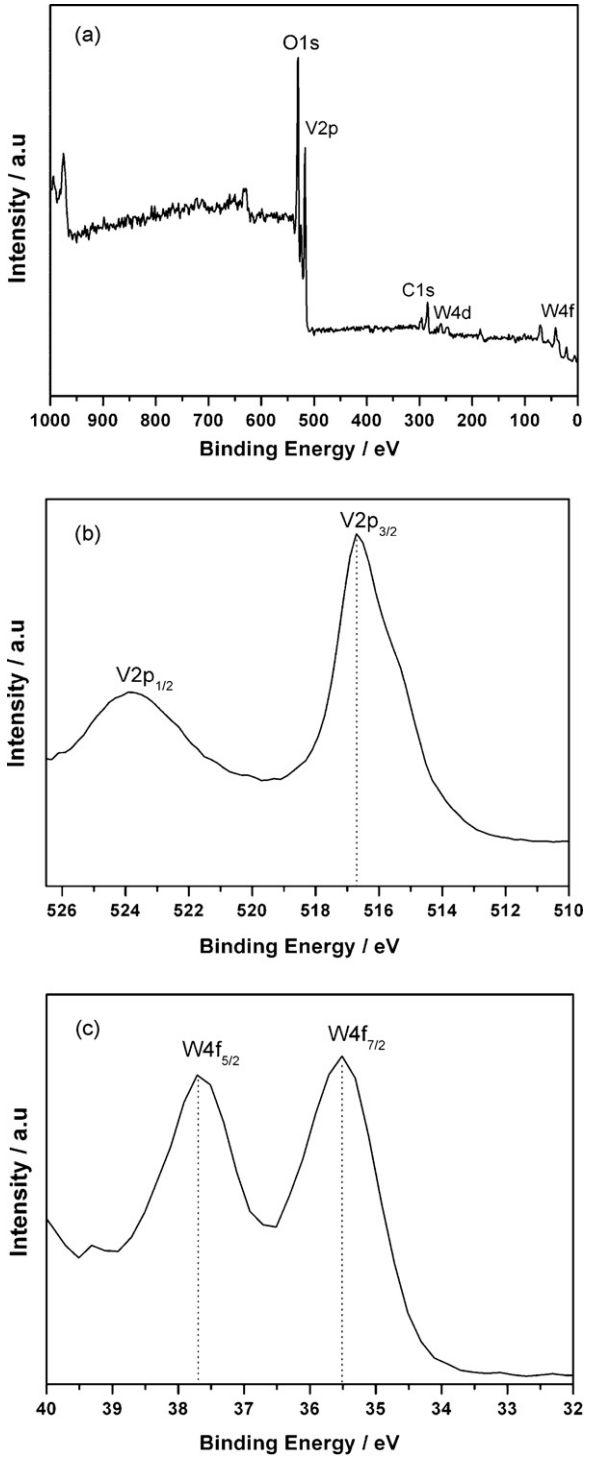

Fig. 4. (a) XPS survey spectrum of W-doped VO_2, (b) V_{2p} peaks of the sample containing 2.13 at %WPTA, (c) W_{4f} peaks of the sample containing 2.13 at% WPTA (calcination condition: 773 K for 0.5 h).

of representative VO_2 powders containing 2.13% amounts of tungsten. The XPS results indicate that there are only four elements: carbon, vanadium, tungsten and oxygen, in the spectrum where carbon peak is from the surface contamination. Peaks at 35.5 eV and 37.7 eV are attributed to $W4f_{7/2}$ and $W4f_{5/2}$ respectively. According to the standard binding energy, it is shown that there is a little tungsten in the sample, and the existent form of tungsten ions in these nanopowders is W^{6+}. The XPS compositional results indicate the successful synthesis of pure W-doped VO_2 particles. Additionally,

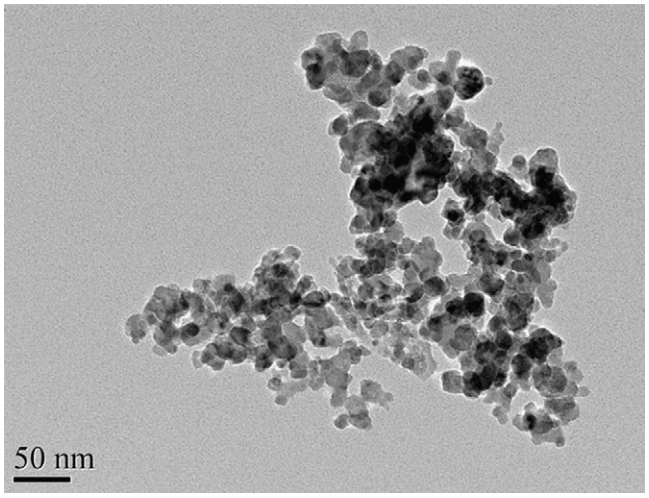

Fig. 5. Transmission electron-microcopy micrographs of W-doped VO_2 nanopowders.

the peak at 516.8 eV due to $V2p_{3/2}$, appearing in the XPS of W-doped VO_2 particles, has the same binding energies of $V_{2p_{3/2}}{}^{4+}$ as reported in literatures [24,25]. This suggests that the valence of vanadium is +4 for both cases and then confirms that the obtained vanadium oxide is stoichiometric and consists of pure VO_2. The powder has a tungsten content of 2.13 at% from XPS data. The other peaks at 529.6 eV and 523.7 eV belong to O_{1s} and $V_{2p_{1/2}}$ respectively.

3.4. Microscopy studies

The sample annealed at 773 K for 0.5 h was placed in absolute alcohol and dispersed by ultrasound for 15 min. The morphology of the powders was directly confirmed by the TEM. Typical TEM images (Fig. 5) shows that the samples display spherical shape with weak agglomeration and narrow size distribution. Primary particles with sizes ranging between 10 nm and 15 nm are found to be linked together. As expected, the observed dimensions of each isolated domains of grain are in good agreement with the values of the mean sizes of crystallites calculated from the X-ray diffraction data.

3.5. FTIR studies

Powders were studied after dispersion in a classical KBr pellet (0.1 wt% of VO_2). VO_2 and KBr powders were carefully mixed in an agate mortar to obtain reproducible dispersion of thermochromic particles. FTIR spectroscopy was performed on the as-prepared VO_2 particles, as illustrated in Fig. 6.

The IR spectra at 293 K and 303 K of VO_2 nanocrystals about 15 nm in size calcined at 723K for 30 min in our work are reported in Fig. 6. It can be found that only the absorption at 10 μm for the nanomaterial did not disappear upon heating. Indeed, some authors have previously observed an additional band at around 10 μm [26]. It is commonly discussed as a result of the partial oxidation of VO_2 powders. The red shift of this absorption band, observed in our nanosized samples, could be attributed to the high specific surface contribution, surface mode contribution (including adsorbed species) or initial step in the oxidation mechanism related to high surface sensitivity of these powders [26].

Fig. 6 confirms the strong reversible metal insulator phase transition modifications observed in transmittance measurements upon heating and cooling. The transmittance of VO_2 is about 98% at 293 K in the semiconducting phase and it is reduced to as low as 6% at 303 K in metal phase at the wavelength of 5 μm. And the difference of the transmittance (ΔT) of these two states is 92%, which

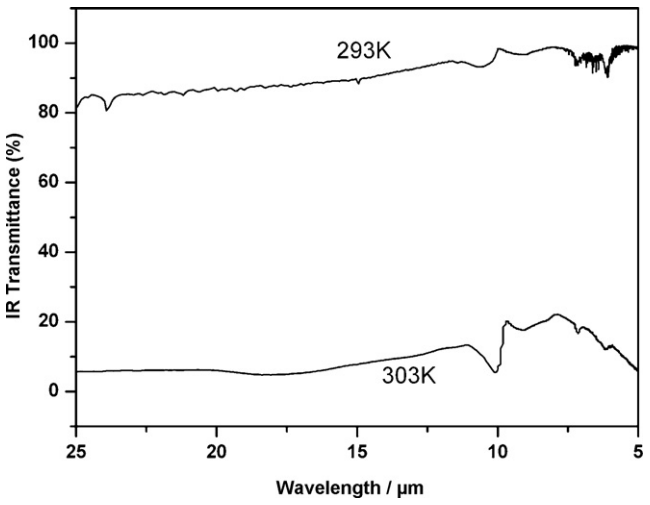

Fig. 6. Fourier transform infrared transmittance spectrum of VO_2 nanopowder dispersed in a classical KBr pellet, in the 25–5 μm range.

is usually sufficient for smart windows and protection of sensitive infrared detectors from strong laser radiation. For nanoparticles, this contrast is maximized at $\lambda = 5\,\mu m$ and no obvious change is found in the 5–25 μm wavelength range with increasing wavelength, which is different from the report that this change would become negligible in the vibrational range ($\lambda > 10\,\mu m$) [27]. It maybe attributed to smaller particles we obtained, for our sample is about 15 nm. The sizes of primary particles can play a prominent role in the final properties of the materials, because the diffusive phenomenon occurs in the MID-infrared range. In fact, in such granular media, the crystal or grain dimensions can play a drastic role in the electrical and optical property. They [28,29] showed that the amplitude of optical contrast in the infrared range could be highly increased by decreasing VO_2 particle sizes. As is well known, diffuse scattering of infrared radiation decreases as particle sizes decrease, because infrared light transmission is strongly increased when particle sizes are smaller than the wavelength of the incident radiation. And nanoparticles of VO_2 [27] could allow minimizing the most part of diffuse scattering phenomena.

4. Conclusions

Well-crystallized and narrow size distribution nanopowders of vanadium dioxide and tungsten-doped vanadium dioxide were successfully synthesized by thermolysis method with white powdery tungstic acid used as a substitutional dopant. The micro-structure was studied in detail by XRD and TEM. A crunode at 8.02% W doping for W-doped VO_2 particles can be observed from XRD with W contents up to 10.03%. According to the curves of DSC, the transition temperature of the W-doped powders is reduced to 298.6K.The transition temperature and IR properties depend on the size, structure, and composition of the nanopowders. The IR properties of the powders change remarkably around the phase-transition temperature, the contrast of semi-metal states is measured being 92%, which is beneficial for the development and application of an intelligent window material.

Acknowledgments

This work is supported by Shanghai Board of Education Fund under contract/grant number CL 200810.We thank Professor Lehan Wei for the supply of a constant current source.

References

[1] F. Guinneton, L. Sauques, J.C. Valmalette, Thin Solid Films 446 (2004) 287.
[2] L.B. Knight Jr., R. Babb, M. Ray, T.J. Banisaukas III, L. Russon, R.S. Dailey, E.R. Davidson, J. Chem. Phys. 105 (1996) 10237.
[3] B.S. Guiton, Q. Gu, L.A. Prieto, M.S. Gudiksen, H. Park, J. Am. Chem. Soc. 127 (2) (2005) 498–499.
[4] F.J. Morin, Phys. Rev. Lett. 3 (1959) 34.
[5] N. Renard, C. Sella, O. Nemraoui, M. Maaza, Y. Sampeur, J. Lafait, Surf. Coat. Technol. 98 (1–3) (1998) 1477.
[6] M. Tazawa, P. Jin, K. Yoshimura, T. Miki, S. Tanemura, Sol. Energy 64 (1–3) (1998) 3.
[7] Z.P. Wu, A. Miyashita, S. Yamamoto, I. Nashiyama, K. Narumi, H. Naramoto, Mater. Construct. 50 (2000) 5–10.
[8] J.S. Hale, J.A. Woollam, Thin Solid Films 339 (1–2) (1999) 174.
[9] C. Alfred-Duplan, J. Musso, J.R. Gavarri, C. Cesari, J. Solid State Chem. 110 (1) (1994) 6.
[10] C.M. Lampert, Solar Energy Mater. 11 (1) (1984) 18.
[11] C.G. Granqvist, Thin Solid Films 193–194 (1990) 730.
[12] M.H. Lee, Sol. Energy Mater. Sol. Cells 71 (2002) 537.
[13] M.H. Lee, J.S. Cho, Thin Solid Films 365 (2000) 5.
[14] C. Reintsema, E. Grossman, J. Koch, SPIE Proc IR Technol. XXV 3698 (1999) 190.
[15] L.A.L. de Almeida, G.S. Deep, A.M.N. Lima, H. Neff, R.C.S. Freire, IEEE Trans. Instrum. Meas. 50 (2001) 1030.
[16] T.E. Phillips, R.A. Murray, T.O. Poelher, Mater. Res. Bull. 22 (1997) 1113.
[17] F. Beteille, R. Morineau, J. Livage, M. Nagano, Mater. Res. Bull. 32 (1997) 1109.
[18] T.D. Manning, I.P. Parkin, M.E. Pemble, D.W. Sheel, D. Vernardou, Chem. Mater. 16 (2004) 744.
[19] J.B. Goodenough, J. Solid State Chem. 3 (1971) 490.
[20] Z.F. Peng, W. Jiang, H. Liu, J. Phys. Chem. C 111 (3) (2007) 1119–1122.
[21] P. Legrand, J.R. Gavarri, J.C. Valmalette, G. Vacquier, J. Lefèvre, US Patent No. 6,358,307.
[22] C. Tang, P. Georgopoulos, M.E. Fine, J.B. Cohen, M. Nygren, G.S. Knapp, A. Aldred, Phys. Rev. B 31 (1985) 1000.
[23] A. Zylbersztein, N.F. Mott, Phys. Rev. B 11 (1975) 4383.
[24] T.D. Manning, I.P. Parkin, M.E. Pemble, D. Sheel, D. Vernardou, Chem. Mater. 16 (2004) 744.
[25] S.W. Lu, L.S. Hou, F.X. Gan, Thin Solid Films 353 (1999) 40.
[26] F. Theobald, Thesis, Besancon University, 1975.
[27] F. Guinneton, J.C. Valmalette, J.R. Gavarri, Opt. Mater. 15 (2000) 111–114.
[28] J.C. Valmalette, J.R. Gavarri, Mater. Sci. Eng. B 54 (1998) 168–173.
[29] J.C. Valmalette, J.R. Gavarri, G. Vacquier, J. Legrand, J. Lefèvre, US Appl. No 08/836,939 (1996).